

AperTO - Archivio Istituzionale Open Access dell'Università di Torino

## Development of sigma-1 ( $\sigma$ 1) receptor fluorescent ligands as versatile tools to study $\sigma$ 1 receptors

### This is the author's manuscript

*Original Citation:*

*Availability:*

This version is available <http://hdl.handle.net/2318/1556537> since 2017-05-13T22:05:47Z

*Published version:*

DOI:10.1016/j.ejmech.2015.12.014

*Terms of use:*

Open Access

Anyone can freely access the full text of works made available as "Open Access". Works made available under a Creative Commons license can be used according to the terms and conditions of said license. Use of all other works requires consent of the right holder (author or publisher) if not exempted from copyright protection by the applicable law.

(Article begins on next page)

# Development of sigma-1 ( $\sigma_1$ ) Receptor Fluorescent Ligands as Versatile Tools to Study $\sigma_1$ Receptors

Carmen Abate,<sup>\*,a</sup> Chiara Riganti,<sup>b</sup> Maria Laura Pati,<sup>a</sup> Dario Ghigo,<sup>b</sup> Francesco Berardi,<sup>a</sup> Timur Mavlyutov,<sup>c</sup> Lian-Wang Guo,<sup>c</sup> Arnold Ruoho<sup>d</sup>

<sup>a</sup>*Dipartimento di Farmacia-Scienze del Farmaco, Università degli Studi di Bari ALDO MORO, Via Orabona 4, I-70125 Bari, Italy*

<sup>b</sup>*Department of Oncology, University of Turin, via Santena 5/bis, 10126, Torino, Italy*

<sup>c</sup>*Department of Surgery, School of Medicine and Public Health, University of Wisconsin, Madison, USA*

<sup>d</sup>*Department of Neuroscience, School of Medicine and Public Health, University of Wisconsin, Madison, USA*

\*To whom correspondence should be addressed. Tel.: +39-080-5442750. Fax.: +39-080-5442231. E-mail: [carmen.abate@uniba.it](mailto:carmen.abate@uniba.it)

## **Abstract**

Despite their controversial physiology, sigma-1 ( $\sigma_1$ ) receptors are intriguing targets for the development of therapeutic agents for central nervous system diseases. With the aim of providing versatile pharmacological tools to study  $\sigma_1$  receptors, we developed three  $\sigma_1$  fluorescent tracers by functionalizing three well characterized  $\sigma_1$  ligands with a fluorescent tag. A good compromise between  $\sigma_1$  binding affinity and fluorescent properties was reached, and the  $\sigma_1$  specific targeting of the novel tracers was demonstrated by different techniques: photolabeling, confocal microscopy and flow cytometry. These novel ligands were also successfully used in competition binding studies by flow cytometry, showing their utility in nonradioactive binding assays as an alternative strategy to the more classical radioligand binding assays. To the best of our knowledge these novel tracers are the first  $\sigma_1$  fluorescent ligands to be developed, and represent promising tools to strengthen  $\sigma_1$  receptors related studies.

## 1. Introduction

The existence of sigma ( $\sigma$ ) receptors was first reported in 1976 when they were considered as subtypes of opiate receptors [1]. Later studies clarified that they are a unique set of proteins divided into two subtypes, namely  $\sigma_1$  and  $\sigma_2$ . The  $\sigma_2$  subtype is the lesser known: it has not yet been cloned, and different hypotheses about its identity have been formulated [3–4]. Despite this paucity of information, interest in  $\sigma_2$  receptor research is on the increase because this subtype is overexpressed in several cancers and its activation through ligands leads cancers cells to death [5–8]. Worthy of note is also the efficacy of  $\sigma_2$  ligands in resistant tumors that shed light on novel strategies for tumor treatments [9]. On the other hand,  $\sigma_1$  receptor was cloned right after the two subtypes were discovered [10, 11]. Several structures were proposed for this 223 amino-acids protein and the most accepted model represents the  $\sigma_1$  receptor made of three hydrophobic regions two of which are trans-membrane spanning segments. The  $\text{NH}_2$  and the  $\text{COOH}$  termini of the  $\sigma_1$  protein are on the same side of the cell compartment where a possible endogenous ligand, not yet identified, regulates its function [12]. Progesterone, sphingolipid-derived amines (*D*-erythro-sphingosine) and more recently *N,N*-dimethyltryptamines have been proposed as  $\sigma_1$  endogenous ligands [13–15]. Because of the important therapeutic potentials (e.g. treatment of anxiety, depression, schizophrenia, etc) linked to  $\sigma_1$  receptor targeting, interest in  $\sigma_1$  receptor research is on the increase [16]. Recent evidence has shown that  $\sigma_1$  receptor can naturally form dimers and/or oligomer and that heteromers between  $\sigma_1$  and  $\text{D}_2$  receptor play an important role in cocaine addiction [17, 18]. These dimers/oligomers may lead to different functional forms of the  $\sigma_1$  receptor (such as agonist or antagonist activity). All these lines of evidence make novel pharmacological tools appealing for the study of the still controversial  $\sigma_1$  receptor physiology. With this aim, we produced three  $\sigma_1$  receptor fluorescent tracers starting from previously well characterized  $\sigma_1$  receptor ligands. We adopted the same strategy that was shown to be successful for  $\sigma_2$  fluorescent ligands: the appropriate  $\sigma_1$  pharmacophore was linked through a spacer to a

green emitting fluorescent tag [19–21]. In particular, as  $\sigma_1$  pharmacophores we selected 4-methyl-1-[4-(6-methoxy-1,2,3,4-tetrahydronaphthalen-1-yl)butyl]piperidine PB190 and 4-methyl-1-[4-(6-methoxy-naphthalen-1-yl)butyl]piperidine PB212 (Figure 1) which were shown to be respectively a  $\sigma_1$  selective agonist and a  $\sigma_1$  selective antagonist by both *in vitro* and *in vivo* assays [22–26]. We also selected 4-cyclohexyl-1-[3-(5-methoxy-1,2,3,4-tetrahydronaphthalen-1-yl)propionyl]piperazine (Figure 1, **1**) which showed excellent  $\sigma_1$  affinity and  $\sigma_1$  vs  $\sigma_2$  selectivity [27]. The methoxy group present in these  $\sigma_1$  ligands was replaced by a hexamethylenoxy chain carrying in the  $\omega$  position a 4-*N,N*-dimethylphthalimide moiety. These choices were made on the basis of data obtained from  $\sigma_2$  receptor fluorescent ligands: the position on the naphthalene or tetralin ring and the nature of the linker showed to be well tolerated with 4-*N,N*-dimethylphthalimide conferring optimal fluorescent properties that allowed successful experiments in living cells by flow cytometry and confocal microscopy.

## 2. Results and Discussion

### 2.1. Chemistry

The synthetic pathway for final compounds **5**, **6** and **9**, is depicted in Scheme 1. The already known piperidines PB190 and PB212 [22] and the piperazine **1** [27] were demethylated by reaction with  $\text{BBr}_3$  to provide the corresponding phenolic intermediates **2**, **3** and **8**, although phenol **3** was previously obtained through another synthetic pathway [28]. Alkylation of the phenolic intermediates **2**, **3** and **8** with the already known mesyl derivative **4** [20] provided final fluorescent compounds **5**, **6** and **9**. Final compounds **6** and **9** were converted into the corresponding hydrochloride salts with gaseous HCl, whereas **5** was converted into the corresponding oxalate salt.

### 2.2. $\sigma$ Receptors Radioligand binding

Results from binding assays are expressed as inhibition constants ( $K_i$  values) in Table 1. As in the  $\sigma_2$  receptors fluorescent ligands, the introduction of the fluorescent tag connected through the hexamethylenoxy linker at the 2- or 5-position of the naphthalene and tetralin ring respectively,

produced a decrease in the  $\sigma_1$  receptor affinity with respect to the corresponding lead compounds. Only compound **5** presented affinity values at both  $\sigma$  receptors ( $K_i = 3.61$  nM at the  $\sigma_1$ , and  $K_i = 48.3$  nM at the  $\sigma_2$ ) comparable to those of lead compound PB190 ( $K_i = 1.01$  nM at the  $\sigma_1$ , and  $K_i = 48.7$  nM at the  $\sigma_2$ ). Final compounds **6** and **9** presented a 100-fold drop in the  $\sigma_1$  affinity ( $K_i = 5.20$  nM and  $K_i = 13.1$  nM, respectively) in comparison to the lead compounds PB212 and **1**, respectively ( $K_i = 0.03$  nM and  $K_i = 0.11$  nM, respectively). By contrast, the affinity at the  $\sigma_2$  receptors only slightly decreased for **6** (2.5-fold) in comparison to its lead compound PB212, whereas  $\sigma_2$  receptor affinity of **9** was 5-fold higher than  $\sigma_2$  receptor affinity displayed by **1**. Despite the decrease in the  $\sigma_1$  affinity compared to the lead compounds, the three fluorescent ligands still demonstrated strong nanomolar  $\sigma_1$  binding, and compounds **5** and **6** also kept a certain  $\sigma_1$  versus  $\sigma_2$  receptor selectivity (10-fold), which was lower (3-fold) in **9**. Taking these data together, the strategy adopted to obtain  $\sigma_2$  receptor fluorescent ligands showed to be successful also for  $\sigma_1$  receptor fluorescent ligands.

**2.3. Photolabeling and Cell Viability Assay.** To demonstrate the universality of specific binding of the novel tracers to  $\sigma_1$  receptors we performed a photolabeling assay, selecting compounds **6** and **9** bearing structurally different basic moieties and using rat adrenal gland pheochromocytoma PC12 cell membranes as a convenient source of  $\sigma_1$  receptors. As shown in Figure 2.A, both **6** and **9** effectively protected against photolabeling of  $\sigma_1$  receptor by [ $^{125}$ I]-Iodoazidophenpropimorph. Further, as shown in Figure 2. B, the cytoprotective properties of compound **9** were assessed in a MTT cell viability assay upon toxicity mediated by paraquat. It is clear that compound **9** protects against such toxicity and therefore may be useful for oxidative stress treatments.

## **2.4. Fluorescent Ligands Studies.**

*2.4.1. Fluorescent Properties.* The fluorescent properties are listed in Table 1. The three compounds displayed very similar maximum excitation wavelength ( $\lambda_{ex} = 390$  nm) and maximum emission wavelength ( $\lambda_{em} \sim 520$  nm), with an important difference between  $\lambda_{ex}$  and  $\lambda_{em}$  (i.e., Stokes shift) in accordance to the spectra recorded for the  $\sigma_2$  ligands with the same fluorescent tag [20, 21].

Measurement of quantum yields (QY) demonstrated the environment sensitive properties (low fluorescence intensity in polar solvent such as EtOH, but high fluorescence in nonpolar solvents such as CHCl<sub>3</sub>), proper for the 4-*N,N*-dimethylphthalimide fluorescent tag, as recorded for  $\sigma_2$  ligands.

#### 2.4.2. Imaging of ARPE19 cells with compound **9** by confocal microscopy.

In Figure 3 the labeling of human retinal pigment epithelia ARPE19 cells with compound **9** shows fluorescent signals in intracellular membranes. The fluorescent signals were protected by PB190, indicating the specificity of binding to  $\sigma$  receptors.

#### 2.4.3 Detection of $\sigma_1$ receptors by flow cytometry.

Cellular up-take of compounds **5** and **6** was studied by flow cytometry in two human breast tumor MCF7 cell lines: MCF7wt and MCF7 $\sigma_1$ . Both these cell lines were thoroughly and previously characterized: the former overexpresses  $\sigma_2$  receptors ( $B_{\max} = 2.02$  pmol/mg protein) [4, 20] whereas  $\sigma_1$  receptors' expression is very low ( $B_{\max} = 0.17$  pmol/mg protein) [4, 29]; the latter is obtained by stable transfection of MCF7 cells with  $\sigma_1$  c-DNA to obtain a good expression of  $\sigma_1$  receptors ( $B_{\max} = 3.45$  pmol/mg protein) [21, 29]. All of the experiments were performed by incubation of the two cell lines for 45 and 75 min with either compound **5** or **6** at 100 nM, as the fluorescence signal increased in a dose-dependent manner, reaching a plateau at 100 nM. Despite their 10-fold  $\sigma_1$  vs  $\sigma_2$  selectivity, compounds **5** and **6** still display  $\sigma_2$  receptor affinity ( $K_i = 48.3$  nM for **5** and  $K_i = 45.6$  nM for **6**). Therefore, the  $\sigma_2$  selective ligand 2-(3-(6,7-dimethoxy-3,4-dihydroisoquinolin-2(1*H*)-yl)propyl)-5-methoxy-3,4-dihydroisoquinolin-1(2*H*)-one **10** [30] ( $K_i = 2435$  nM at the  $\sigma_1$ , and  $K_i = 4.24$  nM at the  $\sigma_2$ ) was used at 10  $\mu$ M to mask the possible fluorescent signal generated by the  $\sigma_2$  targeting of the fluorescent compounds. The  $\sigma_1$  specificity of the fluorescent tracers (100 nM) was demonstrated by comparison of the fluorescent signals by MCF7 $\sigma_1$  and MCF7wt, (Figure 4) upon treatment with (+)-pentazocine and **10**. In MCF7wt cells, where the fluorescence intensity was very low in each experimental condition, no change in the fluorescent signal by either **5** or **6** was detected upon administration of (+)-pentazocine or **10** (Figure 4, right panels). In MCF7 $\sigma_1$  cells the administration of (+)-pentazocine (10  $\mu$ M) strongly decreased the

fluorescent signal by both **5** and **6** (with the signal by **5** completely abated) whereas, treatment with compound **10** (10  $\mu$ M) only slightly decreased fluorescence by both the tracers. As, expected, co-administration of both (+)-pentazocine and **10** completely abated the fluorescent signals by both the tracers (Figure 4, left panels). These results reflected the expression of  $\sigma_1$  receptors in the MCF7 cell lines and suggested that these tracers, administered at 100 nM, bind  $\sigma_1$  receptors rather specifically, with a negligible interference by  $\sigma_2$  receptors. In MCF7 $\sigma_1$ , either **5** (100 nM) or **6** (100 nM) were dose dependently displaced (as demonstrated by the progressive decrease of fluorescence) by pre-incubation with increasing concentrations of either PB190 or PB212 (Figures 5 and 6, A and B; left panels; basal fluorescence of MCF7 cells in the presence of PB190 or PB212 reported in Figure 1 in the supporting information), which were used as  $\sigma_1$  reference non-fluorescent compounds (from 1 nM to 10  $\mu$ M). The same experiment was performed with (+)-pentazocine and a dose-dependent displacement was again recorded, with more linear results obtained by 45 min incubation time (Figure 7). By contrast, no differences were shown between the two incubation times studied (45 min or 75 min) when **5** or **6** were displaced by PB190 and PB212. As expected from a cell line with very low amount of  $\sigma_1$  receptors, the displacement was far more modest in MCFwt (Figures 5–7, A and B; right panels). The fluorescence intensity results obtained by either **5** or **6** in MCF7 $\sigma_1$  cells by dose-dependent displacement of the  $\sigma_1$  receptor ligands studied, served to generate binding curves for PB190, PB212 and (+)-pentazocine allowing the measurement of the IC<sub>50</sub> values of these compounds for the human  $\sigma_1$  receptors in MCF7 cells (Table 2). Differences between radioligand binding assays performed on animal tissues and human cells homogenates have already been reported for  $\sigma_1$  receptors, with slightly lower binding affinities from the latter experiment [31]. The IC<sub>50</sub> values obtained by flow cytometry on MCF7 $\sigma_1$  cells were in accordance with such trend, demonstrating the utility of  $\sigma_1$  receptors fluorescent ligand as tools to detect their presence in living cells and to conveniently perform  $\sigma_1$  binding assays of novel ligands in spite of the radioligand binding assays.

#### 4. Conclusions

Three  $\sigma_1$  fluorescent tracers were synthesized by functionalization of three well characterized  $\sigma_1$  ligands with a fluorescent tag. A good compromise between binding affinity at the  $\sigma_1$  subtype and fluorescent properties was obtained, with all the compounds displaying low nanomolar  $\sigma_1$  receptor affinity. Their  $\sigma_1$  receptor specificity was demonstrated by protection with  $\sigma_1$ -specific compounds in different cell lines through different techniques: photolabeling (compounds **6** and **9**), confocal microscopy (compound **9**) and flow cytometry (compounds **5** and **6**). We also demonstrated that through the use of these fluorescent tracers in flow cytometry,  $\sigma_1$  binding assays of novel ligands can be conveniently performed in spite of the more classical radioligand binding assays that involves the use of radioligands such as [ $^3\text{H}$ ]-(+)-pentazocine. To the best of our knowledge, these compounds are the first  $\sigma_1$  fluorescent ligands to be produced and successfully employed, and they emerge as useful tools to empower  $\sigma_1$  receptors studies.

## 5. Experimental section

**5.1. Chemistry** Both column chromatography and flash column chromatography were performed with 60 Å pore size silica gel as the stationary 300 phase (1:30 w/w, 63–200  $\mu\text{m}$  particle size, from ICN and 1:15 w/w, 15–40  $\mu\text{m}$  particle size, from Merck, respectively). Melting points were determined in open capillaries on a Gallenkamp electrothermal apparatus. Purity of tested compounds was established by combustion analysis, confirming a purity >95%. Elemental analyses (C, H, N) were performed on an Eurovector Euro EA 3000 analyzer; the analytical results were within  $\pm 0.4\%$  of the theoretical values, unless otherwise indicated.  $^1\text{H}$  NMR spectra were recorded on a Mercury Varian 300 MHz using  $\text{CDCl}_3$  as solvent, unless otherwise reported. The following data were reported: chemical shift ( $\delta$ ) in ppm, multiplicity (s, singlet; d, doublet; t, triplet; q, quadruplet; m, multiplet), integration and coupling constants in hertz. Recording of mass spectra was done on an Agilent 6890-5973 MSD gas chromatograph/mass spectrometer and on an Agilent 1100 series LC-MSD trap system VL mass spectrometer; only significant  $m/z$  peaks, with their percentage are

reported in parentheses. Chemicals were from Aldrich, TCI and Alfa Aesar and were used without any further purification.

## 5.2. General procedure for the synthesis of phenolic intermediates (2, 3, 8)

A solution of one among the methoxy derivatives PB190, PB212 and **1** (1.0 mmol) in anhydrous CH<sub>2</sub>Cl<sub>2</sub> (10 mL) and under Argon was cooled to -78 °C and then added in a dropwise manner with BBr<sub>3</sub> (3.0 mmol, 0.3 mL). The mixture was stirred overnight under Argon while it slowly reached room temperature. After cooling in an ice bath, H<sub>2</sub>O was added to the mixture which was basified with Na<sub>2</sub>CO<sub>3</sub>. The resulting mixture was extracted with CH<sub>2</sub>Cl<sub>2</sub> (3 × 10 mL) and the organic phases collected, dried (Na<sub>2</sub>SO<sub>4</sub>) and concentrated under reduced pressure to afford crude oils which provided the title compounds upon purification through column chromatography (CH<sub>2</sub>Cl<sub>2</sub>/MeOH, 95:5).

5.2.1. **5-[4-(4-methylpiperidine-1-yl)butyl]-5,6,7,8-tetrahydronaphthalen-2-ol (2)**: was obtained in 69% yield (0.204 g) as beige solid: mp = 184-186 °C; GS-MS *m/z*: 301 (M<sup>+</sup>, 20), 112 (100); LC-MS (ESI) *m/z*: 300 [M - H]<sup>-</sup>.

5.2.2. **5-[4-(4-methylpiperidine-1-yl)butyl]naphthalen-2-ol (3)**: was obtained in 69% yield (0.202 g) as beige solid: mp = 182-184 °C (literature<sup>[28]</sup> mp = 183-185 °C); GS-MS *m/z*: 297 (M<sup>+</sup>, 20), 112 (100); LC-MS (ESI) *m/z*: 296 [M - H]<sup>-</sup>; LC-MS-MS 296: 156.

5.2.3. **4-Cyclohexyl-1-[3-(5-hydroxy-1,2,3,4-tetrahydronaphthalen-1-yl)propionyl]piperazine (8)**: was obtained in 90% yield (0.33 g) as sticky solid. <sup>1</sup>H-NMR δ 1.05-1.35 [m, 6H, cyclohexyl], 1.55-2.05 (m, 10H, COCH<sub>2</sub>CH<sub>2</sub>CHCH<sub>2</sub>CH<sub>2</sub> and cyclohexyl CH<sub>2</sub>), 2.20 - 2.45 (m, 3H, benzyl CH and CH<sub>2</sub>), 2.50-2.58 (m, 4H, CH<sub>2</sub> piperazine), 2.60-2.75 (m, 2H, CH<sub>2</sub>CO), 2.80-2.85 (m, 1H, CHN), 4.38-4.70 [m, 4H, CON(CH<sub>2</sub>)<sub>2</sub>], 5.20 (broad s, 1H, OH), 6.60 (d, *J* = 7.15 Hz, 1H aromatic), 6.78 (d, *J* = 7.7 Hz, 1H, aromatic), 7.00 (t, *J* = 7.8 Hz, 1H, aromatic); GS-MS *m/z*: 370 (M<sup>+</sup>, 30), 138 (70), 125 (100), 112 (80).

## 5.3. General procedure for the synthesis of final fluorescent compounds (5, 6 and 9).

A solution in DMF (10 mL) of one among the phenol intermediates **2** or **3** or **8** (1.0 mmol) was added with the mesyl derivative **4** (1.0 mmol, 0.37 g) and K<sub>2</sub>CO<sub>3</sub> (1.2 mmol, 0.16 g) to provide a mixture which was stirred at 150 °C overnight. After concentration under reduced pressure the crude residue which was taken up with water was extracted with CH<sub>2</sub>Cl<sub>2</sub> (3 × 10 mL) and the organic phases collected were dried (Na<sub>2</sub>SO<sub>4</sub>) and evaporated under reduced pressure to provide a crude oil which was purified by column chromatography (CH<sub>2</sub>Cl<sub>2</sub>/MeOH, 95:5) to afford the title compounds.

5.3.1. **5-(dimethylamino)-2-(6-((5-(4-(4-methylpiperidin-1-yl)butyl)-5,6,7,8-tetrahydronaphthalen-2-yl)oxy)hexyl)isoindoline-1,3-dione. (5)** The title compound was obtained in a 50% yield (0.286 g) as a bright yellow oil. <sup>1</sup>H-NMR δ 0.98 (d, *J* = 5.7 Hz, 3H, CHCH<sub>3</sub>), 1.25-2.00 [m, 19H, N(CH<sub>2</sub>)<sub>2</sub>, CH<sub>2</sub>(CH<sub>2</sub>)<sub>4</sub>, CH(CH<sub>2</sub>)<sub>3</sub> e NH], 2.25-2.40 (m, 3H, benzyl CH and CH<sub>2</sub>), 2.60-2.70 (m, 4H, N(CHH)<sub>2</sub> and CH<sub>2</sub>CH<sub>2</sub>CH<sub>2</sub>N), 2.85-2.95 (m, 2H, N(CHH)<sub>2</sub>), 3.10 [s, 6H, N(CH<sub>3</sub>)<sub>2</sub>], 3.62 (t, *J* = 7.15 Hz, 2H, (CO)<sub>2</sub>NCH<sub>2</sub>), 3.88 (t, *J* = 6.6 Hz, 2H, OCH<sub>2</sub>), 6.50-7.65 (m, 6H, aromatic); LC-MS (ESI<sup>+</sup>) *m/z*: 574 [M + H]<sup>+</sup>; LC-MS-MS 574: 203. Anal. (C<sub>36</sub>H<sub>51</sub>N<sub>3</sub>O<sub>3</sub>·C<sub>2</sub>O<sub>4</sub>H<sub>2</sub>·½H<sub>2</sub>O) C, H, N.

5.3.2. **5-(dimethylamino)-2-{6-[(5-(4-(4-methylpiperidin-1-yl)butyl)naphthalen-2-yl)oxy]hexyl}isoindole-1,3-dione (6).** The title compound was obtained in a 50% yield (0.284 g) as a bright yellow oil. <sup>1</sup>H-NMR δ 0.95-1.00 (m, 3H, NHCH<sub>3</sub>), 1.15-2.05 [m, 17H, CH(CH<sub>2</sub>)<sub>2</sub>, (CO)<sub>2</sub>NCH<sub>2</sub>(CH<sub>2</sub>)<sub>4</sub>CH<sub>2</sub> and ArCH<sub>2</sub>(CH<sub>2</sub>)<sub>2</sub>], 2.60-2.75 [m, 2H, N(CHH)<sub>2</sub>], 2.85-2.95 [m, 2H, N(CHH)<sub>2</sub>], 2.98-3.05 [m, 4H, Ar(CH<sub>2</sub>)<sub>3</sub>CH<sub>2</sub>N], 3.10 [s, 6H, N(CH<sub>3</sub>)<sub>2</sub>], 3.65 (t, *J* = 7.15 Hz, 2H, (CO)<sub>2</sub>NCH<sub>2</sub>), 4.05 (t, *J* = 6.6 Hz, 2H, OCH<sub>2</sub>), 6.70-8.05 (m, 9H, aromatic); LC-MS (ESI<sup>+</sup>) *m/z*: 570 [M + H]<sup>+</sup>; LC-MS-MS 570: 203. Anal. (C<sub>36</sub>H<sub>47</sub>N<sub>3</sub>O<sub>3</sub>·HCl·1.75H<sub>2</sub>O) C, H, N.

5.3.3. **2-(6-((5-(3-(4-cyclohexylpiperazin-1-yl)-3-oxopropyl)-5,6,7,8-tetrahydronaphthalen-1-yl)oxy)hexyl)-5-(dimethylamino)isoindole-1,3-dione (8).** The title compound was obtained in a 57% yield as a yellow oil (0.366 g). <sup>1</sup>H-NMR δ 1.05-2.05 [m, 24H, piperazine CH<sub>2</sub>, OCH<sub>2</sub>(CH<sub>2</sub>)<sub>4</sub>, CH(CH<sub>2</sub>)<sub>3</sub>], 2.20-2.85 [m, 10H, CHN(CH<sub>2</sub>)<sub>2</sub>, CH<sub>2</sub>CO, benzyl CH and CH<sub>2</sub>], 3.11 [s, 6H, (NCH<sub>3</sub>)<sub>2</sub>], 3.38-3.42 [m, 2H, CON(CHH)<sub>2</sub>], 3.58-3.45 [m, 4H, (CO)<sub>2</sub>NCH<sub>2</sub> and CON(CHH)<sub>2</sub>], 3.90 (t, 2H, *J* =

6.1 Hz, OCH<sub>2</sub>), 6.60-6.65 (m, 6H, aromatic); LC-MS (ESI<sup>+</sup>) *m/z*: 665 [M + Na]<sup>+</sup>; LC-MS-MS 665: 497, 393. Anal. (C<sub>39</sub>H<sub>54</sub>N<sub>4</sub>O<sub>4</sub>·2HCl) C, H, N.

## 5.4. Biology

5.4.1. *Materials*. [<sup>3</sup>H]-DTG (50 Ci/mmol), and (+)-[<sup>3</sup>H]-pentazocine (30 Ci/mmol) were purchased from PerkinElmer Life and Analytical Sciences (Boston, MA). DTG was purchased from Tocris Cookson Ltd., U.K. (+)-Pentazocine was obtained from Sigma–Aldrich (Milan, Italy). Male Dunkin guinea pigs and Wistar Hannover rats (250–300 g) were from Harlan, Italy. Cell culture reagents were purchased from EuroClone (Milan, Italy).

5.4.2. *Competition Binding Assays*. All the procedures for the binding assays were previously described.  $\sigma_1$  And  $\sigma_2$  receptor binding were carried out according to Berardi et al. [27]. [<sup>3</sup>H]-DTG, 1,3-di-2-tolylguanidine (30 Ci/mmol) and (+)-[<sup>3</sup>H]-pentazocine (34 Ci/mmol) were purchased from PerkinElmer Life Sciences (Zavantem, Belgium). DTG was purchased from Tocris Cookson Ltd. (UK). (+)-Pentazocine was obtained from Sigma–Aldrich-RBI s.r.l. (Milan, Italy). Male Dunkin guinea pigs and Wistar Hannover rats (250–300 g) were from Harlan (Italy). The specific radioligands and tissue sources were, respectively: (a)  $\sigma_1$  receptor, (+)-[<sup>3</sup>H]-pentazocine, guinea pig brain membranes without cerebellum; (b)  $\sigma_2$  receptor, [<sup>3</sup>H]-DTG in the presence of 1  $\mu$ m (+)-pentazocine to mask  $\sigma_1$  receptors, rat liver membranes. The following compounds were used to define the specific binding reported in parentheses: (a) (+)-pentazocine (73–87 %), (b) DTG (85–96 %). Concentrations required to inhibit 50% of radioligand specific binding (IC<sub>50</sub>) were determined using six to nine different concentrations of the drug studied in two or three experiments with samples in duplicate. Scatchard parameters ( $K_d$  and  $B_{max}$ ) and apparent inhibition constants ( $K_i$  values) were determined by nonlinear curve fitting, using Prism GraphPad software (version 3.0) [32].

5.4.3. *Cell Culture*. Human breast adenocarcinoma cell line (MCF7) was purchased from ICLC (Genoa, Italy), and were stably transfected with  $\sigma_1$ -receptor c-DNA (MCF7 $\sigma_1$ ) as already described. Cells were grown in DMEM high-glucose medium supplemented with fetal bovine serum (10 %), and penicillin-streptomycin (1%) in a humidified incubator at 37 °C with a CO<sub>2</sub> atmosphere. Human

retinal pigment epithelia ARPE19 cells were purchased from ATCC and grown in complete growth medium (DMEM supplemented with fetal bovine serum 10%) and penicillin-streptomycin (1%) in cell culture incubator with 5% CO<sub>2</sub>. Mouse Motor Neuron NSC34 cells were purchased from Cedarlane company, Canada and were grown in 15 cm cell culture dishes in 50%/50% DMEM/F12 supplemented with 10% fetal bovine serum and 1× penicillin-streptomycin (final 100 µg/ml). Rat adrenal gland pheochromocytoma PC12 cells were purchased from ATCC and were grown in RPMI 1640 (Mediatech) supplemented with 10% heat-inactivated Horse serum (Corning), 5% fetal bovine serum, and penicillin-streptomycin (1%).

*5.4.4. ARPE19 Cell labeling and imaging.* Drug treatment and imaging of ARPE cells was done in HBSS. For control, some wells were pretreated with 100 µM PB190 for 40 min. Cells were further treated with compound **9** 0.5 µM for 40 min, then rinsed twice in HBSS and imaged under A1 confocal microscope with excitation wavelength of 408 nM and emission detection of 525 nM.

*5.4.5. MTT cell viability assay.*

ARPE 19 cells were seeded to 96 well plates to a density of 30000 cells/well and grown in complete growth medium to reach 100% confluency. Then 1 mM toxin Paraquat was applied with or without various concentrations of compound **9** and cells were incubated for 24 h in complete growth media. Then wells were quickly aspirated and Thiazolyl Blue Tetrazolium Bromide (MTT, Sigma-Aldrich M2128) was applied under the dim light at concentration 0.5 mg/ml in phenol red free DMEM (100 µl/well) supplemented with fetal bovine serum 0.5%. After 3 hours of incubation 100 µl of 10% Sodium Dodecyl Sulfate (SDS) was added per each well. Plates were left overnight in cell culture incubator to dissolve precipitate. Absorbance at  $\lambda = 540$  nM was detected in 96 well plate reader.

*5.4.6. Photolabeling experiment.* NSC34 cells and PC12 cells were grown on 15 cm cell culture dishes in complete growth medium. Cells were rinsed with DPBS and detached with cell culture scraper and collected into 15 ml falcon tubes, spun 1000 rpm for 3 min. Pellet was gently rinsed with PBS, cells resuspended, sonicated and spun at 5000G. Soluble fraction was collected and spun at 100000G. Soluble fraction was discarded and translucent pellet was resuspended by sonication on ice. The protein concentration was

measured by the Bradford Bio-Rad assay. For photolabeling, each sample contained 100  $\mu\text{l}$  of 5  $\mu\text{g}/\mu\text{l}$  protein. Where applicable, (+)-pentazocine, DTG were preincubated with the homogenate for 30 min at room temperature. Then carrier-free [ $^{125}\text{I}$ ]-IAF [33] (approximately 1 nM) was added for 30 min, and the membrane preparations were further incubated in the dark at room temperature. After incubation, the samples were illuminated with an AH-6 mercury lamp for 7.5 s, and Laemmli buffer was added to each sample. Samples were separated by SDS PAGE, the gel was stained and dried, and exposed to a phosphor screen (Molecular Dynamics) for 24 h. The cassette was scanned on a Storm Phosphoimager (Molecular Dynamics) to produce the resulting autoradiogram.

*5.4.7. Flow cytometry studies.* MCF7 and MCF7 $\sigma_1$  cells were incubated with increasing concentrations (0.1, 1, 10, and 100 nmol/L and 1 and 10  $\mu\text{mol}/\text{L}$ ) of either PB190 or PB212 followed by 100 nmol/L of either compounds **5** or **6** for 45 or 75 min at 37  $^{\circ}\text{C}$ . To mask  $\sigma_2$  receptors, compound **10** (10  $\mu\text{mol}/\text{L}$ ) was co-incubated. When indicated, cells were treated with increasing concentrations (1, 10, and 100 nmol/L and 1 and 10  $\mu\text{mol}/\text{L}$ ) of (+)-pentazocine or PB190 or PB212, followed by 100 nmol/L of compounds **5** or **6** for 45 or 75 min at 37  $^{\circ}\text{C}$ . At the end of the incubation periods, cells were washed twice with PBS, detached with 200  $\mu\text{l}$  of Cell Dissociation Solution (Sigma Chemical Co.) for 10 min at 37 $^{\circ}\text{C}$ , centrifuged at 13,000  $\times g$  for 5 min and re-suspended in 500  $\mu\text{L}$  of PBS. The fluorescence was recorded using a Bio-Guava® easyCyte™ 5 Flow Cytometry System (Millipore, Billerica, MA), with a 530 nm band pass filter. For each analysis, 50,000 events were collected and analysed with the InCyte software (Millipore).

**5.5. Fluorescence Spectroscopy.** Emission and excitation spectra of compounds **5**, **6** and **9**, were determined in  $\text{CHCl}_3$  and in PBS buffer solution as previously reported. Fluorescence quantum yields were calculated with respect to quinine sulfate as previously reported [19].

**Abbreviations:** DTG, di-2-tolylguanidine; DMEM, Dulbecco's modified Eagle's medium; PBS, phosphate buffered saline; SDS, Sodium Dodecyl Sulfate.

## References

- [1] W.R. Martin, C.G. Eades, J.A. Thompson, R.E. Huppler, P.E. Gilbert, The effect of morphine- and nalorphine-like drugs in the nondependent and morphine-dependent chronic spinal dog, *J. Pharmacol. Exp. Ther.* 197 (1976) 517–532.
- [2] N.A. Colabufo, F. Berardi, C. Abate, M. Contino, M. Niso, R. Perrone, Is the  $\sigma_2$  receptor a histone binding protein?, *J. Med. Chem.* 49 (2006) 4153–4158.
- [3] J. Xu, C. Zeng, W. Chu, F. Pan, J.M. Rothfuss, F. Zhang, Z. Tu, D. Zhou, D. Zeng, S. Vangveravong, F. Johnston, D. Spitzer, K.C. Chang, R.S. Hotchkiss, W.G. Hawkins, K.T. Wheeler, R.H. Mach, Identification of the PGRMC1 protein complex as the putative sigma-2 receptor binding site, *Nat. Commun.* 2 (2011) 380.
- [4] C. Abate, M. Niso, V. Infantino, A. Menga, F. Berardi, Elements in support of the 'non-identity' of the PGRMC1 protein with the  $\sigma_2$  receptor, *Eur J Pharmacol.* 758 (2015) 16–23.
- [5] C. Zeng, J. Rothfuss, J. Zhang, W. Chu, S. Vangveravong, Z. Tu, F. Pan, K.C. Chang, R. Hotchkiss, R.H. Mach, Sigma-2 ligands induce tumour cell death by multiple signalling pathways, *Br. J. Cancer* 106 (2012) 693–701.
- [6] J.R. Hornick, S. Vangveravong, D. Spitzer, C. Abate, F. Berardi, P. Goedegebuure, R.H. Mach, W.G. Hawkins, Lysosomal membrane permeabilization is an early event in Sigma-2 receptor ligand mediated cell death in pancreatic cancer, *J. Exp. Clin. Cancer Res.* 31 (2012) 41.
- [7] C. Abate, R. Perrone, F. Berardi. Classes of sigma2 ( $\sigma_2$ ) receptor ligands: structure affinity relationship (SAfiR) studies and antiproliferative activity. *Curr. Pharm. Des.* 18 (2012) 18 938–949.
- [8] C. Abate, M. Niso, M. Contino, N.A. Colabufo, S. Ferorelli, R. Perrone, F. Berardi, 1-Cyclohexyl-4-(4-arylcyclohexyl)piperazines: mixed  $\sigma$  and human  $\Delta_8$ – $\Delta_7$  sterol isomerase ligands with antiproliferative and P-glycoprotein inhibitory activity, *Chem. Med. Chem.* 6 (2011) 73–80.
- [9] M. Niso, C. Abate, M. Contino, S. Ferorelli, A. Azzariti, R. Perrone, N.A. Colabufo, F. Berardi, Sigma-2 receptor agonists as possible antitumor agents in resistant tumors: hints for collateral sensitivity, *Chem. Med. Chem.* 8 (2013) 2026–2035.

- [10] R. Quirion, W.D. Bowen, Y. Itzhak, J.L. Junien, J.M. Musacchio, R.B. Rothman, T.P. Su, S.W. Tam, D.P. Taylor, A proposal for the classification of sigma binding sites, *Trends Pharmacol. Sci.* 13 (1992) 85–86.
- [11] M. Hanner, F.F. Moebius, A. Flandorfer, H.G. Knaus, J. Striessnig, E. Kempner, H. Glossmann, Purification, molecular cloning, and expression of the mammalian sigma1-binding site, *Proc. Natl. Acad. Sci.* 93 (1996) 8072–8077.
- [12] A. Pal, U.B. Chu, S. Ramachandran, D. Grawoig, L.W. Guo, A.R. Hajipour, A.E. Ruoho, Juxtaposition of the steroid binding domain-like I and II regions constitutes a ligand binding site in the sigma-1 receptor, *J. Biol. Chem.* 283 (2008) 19646–19656.
- [13] M. Johannessen, D. Fontanilla, T. Mavlyutov, A.E. Ruoho, M.B. Jackson, Antagonist action of progesterone at  $\sigma$ -receptors in the modulation of voltage-gated sodium channels, *Am. J. Physiol. Cell Physiol.* 300 (2011) 328–337.
- [14] A.E. Ruoho, U.B. Chu, S. Ramachandran, D. Fontanilla, T. Mavlyutov, A.R. Hajipour, The ligand binding region of the sigma-1 receptor: studies utilizing photoaffinity probes, sphingosine and N-alkylamines. *Curr. Pharm. Des.* 18 (2012) 920-929.
- [15] D. Fontanilla, M. Johannessen, A.R. Hajipour, N.V. Cozzi, M.B. Jackson, A.E. Ruoho. The hallucinogen N,N-dimethyltryptamine (DMT) is an endogenous sigma-1 receptor regulator, *Science* 323 (2009) 934–937.
- [16] S.D. Banister, M. Kassious, The therapeutic potential of sigma receptor for the treatment of central nervous system diseases: evaluation of the evidence, *Curr. Pharm. Des.* 18 (2012) 884-901.
- [17] U.B. Chu, S. Ramachandran, A.R. Hajipour, A.E. Ruoho, Photoaffinity labeling of the sigma-1 receptor with *N*-[3-(4-nitrophenyl)propyl]-*N*-dodecylamine: evidence of receptor dimers. *Biochemistry* 52 (2013) 859–868.
- [18] G. Navarro, E. Moreno, J. Bonaventura, M. Brugarolas, D. Farré, D. Aguinaga, J. Mallol, A. Cortés, V. Casado, C. Lluís, S. Ferre, R. Franco, E. Canela, P.J. McCormick, Cocaine inhibits dopamine D2 receptor signaling via sigma-1-D2 receptor heteromers, *PLoS One* 8 (2013)61245.

- [19] C. Abate, J.R. Hornick, D. Spitzer, W.J. Hawkins, M. Niso, R. Perrone, F. Berardi, Fluorescent derivatives of  $\sigma$  receptor ligand 1-cyclohexyl-4-[3-(5-methoxy-1,2,3,4-tetrahydronaphthalen-1-yl)-propyl]piperazine (PB28) as a tool for uptake and cellular localization studies in pancreatic tumor cells. *J. Med. Chem.* 54 (2011) 5858–5867.
- [20] C. Abate, M. Niso, R. Marottoli, C. Riganti, D. Ghigo, S. Ferorelli, G. Ossato, R. Perrone, E. Lacivita, D.C. Lamb, F. Berardi, Novel derivatives of 1-cyclohexyl-4-[3-(5-methoxy-1,2,3,4-tetrahydronaphthalen-1-yl)propyl]piperazine (PB28) with improved fluorescent and  $\sigma$  receptors binding properties, *J. Med. Chem.* 57 (2014) 3314–3323.
- [21] M. Niso, C. Riganti, M.L. Pati, D. Ghigo, F. Berardi, C. Abate, Novel and selective fluorescent  $\sigma_2$ -receptor ligand with a 3,4-dihydroisoquinolin-1-one scaffold: a tool to study  $\sigma_2$  receptors in living Cells, *Chem. Bio. Chem.* 16 (2015) 1078-1083.
- [22] F. Berardi, S. Ferorelli, C. Abate, M.P. Pedone, N.A. Colabufo, M. Contino, R. Perrone, Methyl substitution on the piperidine ring of *N*-[ $\omega$ -(6-methoxynaphthalen-1-yl)alkyl] derivatives as a probe for selective binding and activity at the  $\sigma_1$  receptor, *J. Med. Chem.* 48 (2005) 8237–8244.
- [23] G. Gasparre, C. Abate, F. Berardi, G. Cassano, The sigma-1 receptor antagonist PB212 reduces the  $\text{Ca}^{2+}$ -release through the inositol (1,4,5)-trisphosphate receptor in SK-N-SH cells. *Eur. J. Pharmacol.* 684 (2012) 59–63.
- [24] G. Skuza, M. Szymanska, B. Budziszewska, C. Abate, F. Berardi, Effects of PB190 and PB212, new  $\sigma$  receptor ligands, on glucocorticoid receptor-mediated gene transcription in LMCAT cells, *Pharmacol. Rep.* 63 (2011) 1564–1568.
- [25] G. Skuza, W. Sadaj, M. Kabzinski, G. Cassano, G. Gasparre, C. Abate, The effects of new sigma ( $\sigma$ ) receptor ligands, PB190 and PB212, in the models predictive of antidepressant activity, *Pharmacol. Rep.* 66 (2014) 320–324.
- [26] C. Moritz, F. Berardi, C. Abate, F. Peri, Live imaging reveals a new role for the sigma-1 ( $\sigma_1$ ) receptor in allowing microglia to leave brain injuries. *Neuroscience Lett.* (2015, 591, 13-18.

- [27] F. Berardi, C. Abate, S. Ferorelli, V. Uricchio, N.A. Colabufo, M. Niso, R. Perrone. Exploring the importance of piperazine N-atoms for  $\sigma_2$  receptor affinity and activity in a series of analogs of 1-cyclohexyl-4-[3-(5-methoxy-1,2,3,4-tetrahydronaphthalen-1-yl)propyl]piperazine (PB28), *J. Med. Chem.* 52 (2009) 7817–7828.
- [28] M. Gao, M. Wang, G.D. Hutchins, Q.H. Zheng, Synthesis of carbon-11-labeled piperidine ring of *N*-[ $\omega$ -(6-methoxynaphthalen-1-yl)alkyl] derivatives as new selective PET  $\sigma_1$  receptor probes, *Appl. Radiat. Isot.* 68 (2010) 459–465.
- [29] C. Abate, S. Ferorelli, M. Niso, C. Lovicario, V. Infantino, P. Convertini, R. Perrone, F. Berardi. 2-Aminopyridine derivatives as potential  $\sigma_2$  receptor antagonists. *ChemMedChem* 2012, 7, 1847–1857.
- [30] C. Abate, S.V. Selivanova, A. Müller, S.D. Krämer, R. Schibli, R. Marottoli, R. Perrone, F. Berardi, M. Niso, S.M. Ametamey, Development of 3,4-dihydroisoquinolin-1(2*H*)-one derivatives for the Positron Emission Tomography (PET) imaging of  $\sigma_2$  receptors, *Eur. J. Med. Chem.* 69 (2013) 920–930.
- [31] F. Berardi, C. Abate, S. Ferorelli, N.A. Colabufo, R. Perrone, 1-Cyclohexylpiperazine and 3,3-dimethylpiperidine derivatives as sigma-1 and sigma-2 receptor ligands: a review. *Cent. Nerv. Syst. Agents Med. Chem.* 9 (2009) 205–219.
- [32] Prism Software, version 3.0 for Windows; GraphPad Software, Inc.: San Diego, CA, 1998.
- [33] A. Pal, A.R. Hajipour, D. Fontanilla, S. Ramachandran, U.B. Chu, T. Mavlyutov, A.E. Ruoho, Identification of regions of the sigma-1 receptor ligand binding site using a novel photoprobe, *Mol Pharmacol.* 72 (2007), 921–933.

**Table 1.**  $\sigma$  Receptor Affinities of Final and Lead-Compounds and Fluorescence Properties.

compound	$K_i$ nM $\pm$ SEM (nM) <sup>[a]</sup>		$\lambda_{\text{ex}}$ nm <sup>[b]</sup>	$\lambda_{\text{em}}$ nm <sup>[b]</sup>	QY EtOH <sup>[c]</sup>	QY CHCl <sub>3</sub> <sup>[c]</sup>
	$\sigma_1$	$\sigma_2$				
<b>PB190</b> <sup>[d]</sup>	1.01 $\pm$ 0.41	48.7 $\pm$ 9.2				
<b>PB212</b> <sup>[d]</sup>	0.03 $\pm$ 0.013	17.9 $\pm$ 5.3				
<b>1</b> <sup>[e]</sup>	0.11 $\pm$ 0.01	179 $\pm$ 56				
<b>5</b>	3.61 $\pm$ 0.4	48.3 $\pm$ 6.0	390	510	0.02	0.5
<b>6</b>	5.20 $\pm$ 0.17	45.6 $\pm$ 4.6	390	520	0.02	0.4
<b>9</b>	13.1 $\pm$ 5.02	38.4 $\pm$ 10.9	390	520	0.02	0.4
<b>DTG</b>		35.4 $\pm$ 5.8				
(+)-pentazocine	4.52 $\pm$ 0.7					

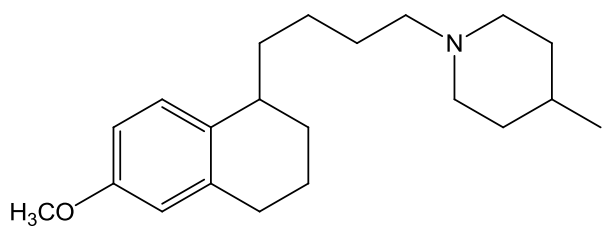
[a] Values are the means of  $n \geq 3$  separate experiments, in duplicate. [b] Fluorescence properties of compounds were evaluated on compound as free base in EtOH solutions. [c] QY were evaluated as in 20; [d] Data from ref 22; [e] Data from ref 27.

**Table 2.**  $\sigma_1$  Receptor Affinities of Reference  $\sigma_1$  Receptor ligands by flow-cytometry with novel  $\sigma_1$  fluorescent ligands.

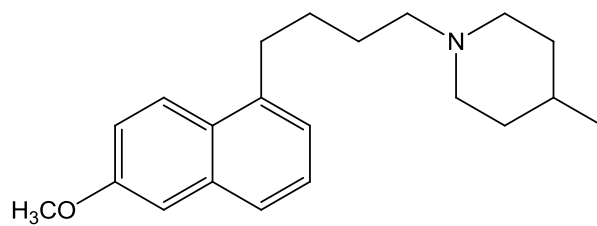
compound	$\sigma_1$ ; IC <sub>50</sub> nM $\pm$ SEM <sup>[a]</sup>	
	<b>5</b> <sup>[b]</sup>	<b>6</b> <sup>[b]</sup>
<b>PB190</b> <sup>[c]</sup>	11.3 $\pm$ 2.4	12.1 $\pm$ 1.4
<b>PB212</b> <sup>[c]</sup>	15.5 $\pm$ 2.3	10.6 $\pm$ 1.2
<b>(+)-pentazocine</b> <sup>[d]</sup>	8.24 $\pm$ 1.2	7.59 $\pm$ 0.8

[a] Values are the means of  $n \geq 2$  separate experiments, in duplicate. [b] IC<sub>50</sub> values from binding curves obtained by dose dependent displacement of **5** (100 nM) or **6** (100 nM) by  $\sigma_1$  reference compounds (PB190, PB212 and (+)-pentazocine) in MCF7 $\sigma_1$  cells by flow cytometry. [c] Data from 75 min incubation time. [d] Data from 45 min incubation time. The experiments were performed in the presence of the  $\sigma_2$  masking agent **10** (10  $\mu$ M).

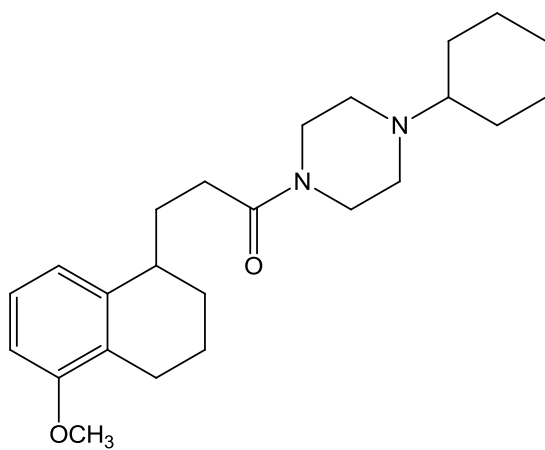
**Figure 1.**



**PB190**



**PB212**



**1**

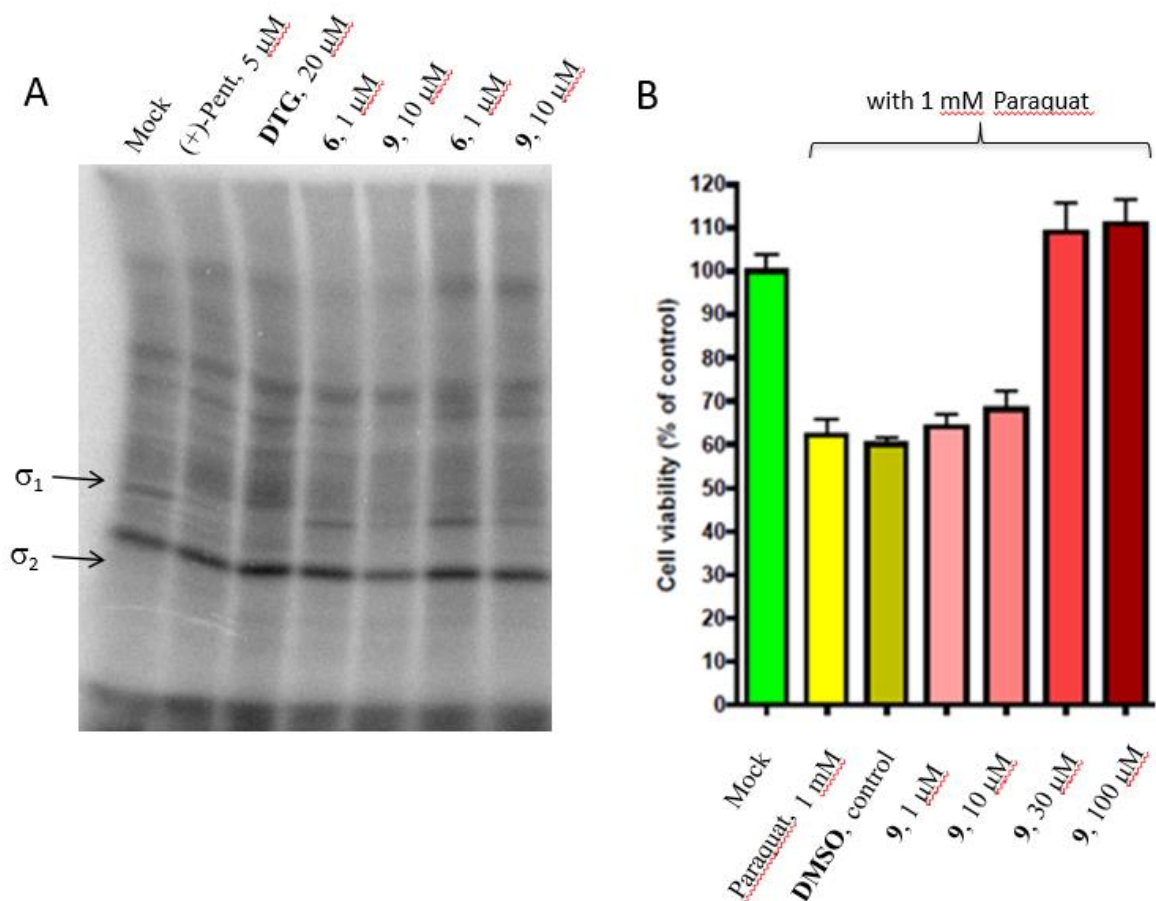


**Figure 2.** Compounds **6** and **9** protected  $\sigma_1$  receptor photolabeling by [ $^{125}$ I]-Iodoazidophenpropimorph and also protected against paraquat-mediated toxicity. A. Photolabeling by [ $^{125}$ I]-Iodoazidophenpropimorph in PC12 cell membranes. 5  $\mu$ M (+)-Pentazocine [(+)-Pent] and di-2-tolylguanidine (DTG) specifically protected the  $\sigma_1$  receptor band. PC12 cells were used as a convenient source of  $\sigma_1$  receptor to show that both compounds **6** and **9** protected  $\sigma_1$  receptor photolabeling. B. Compound **9** in concentration-dependent manner protects against paraquat-mediated toxicity as estimated by a MTT assay in ARPE19 cells. All drugs were applied simultaneously for 24 hours.

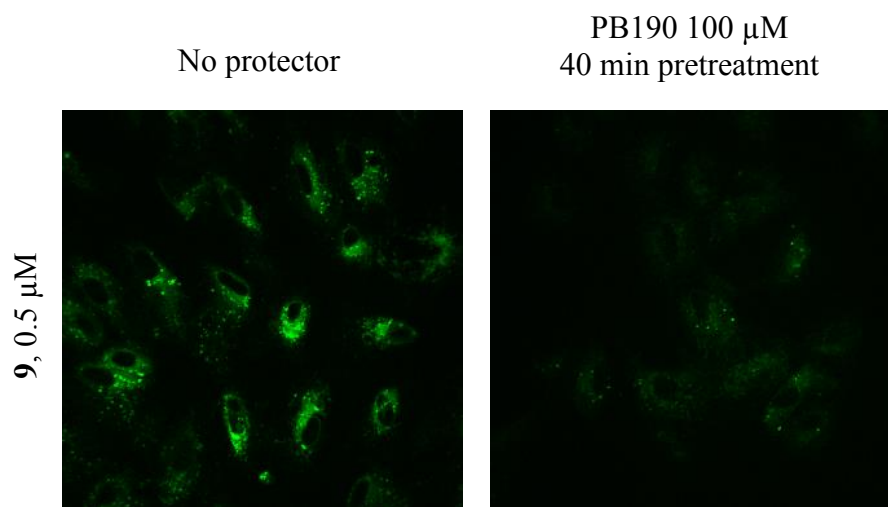


**Figure 3. Labeling of ARPE19 Cells with compound 9.** Signal is localized to intracellular membranes. Lower intensity of labeling is detected when cells were pre-labeled with PB190 100  $\mu$ M.

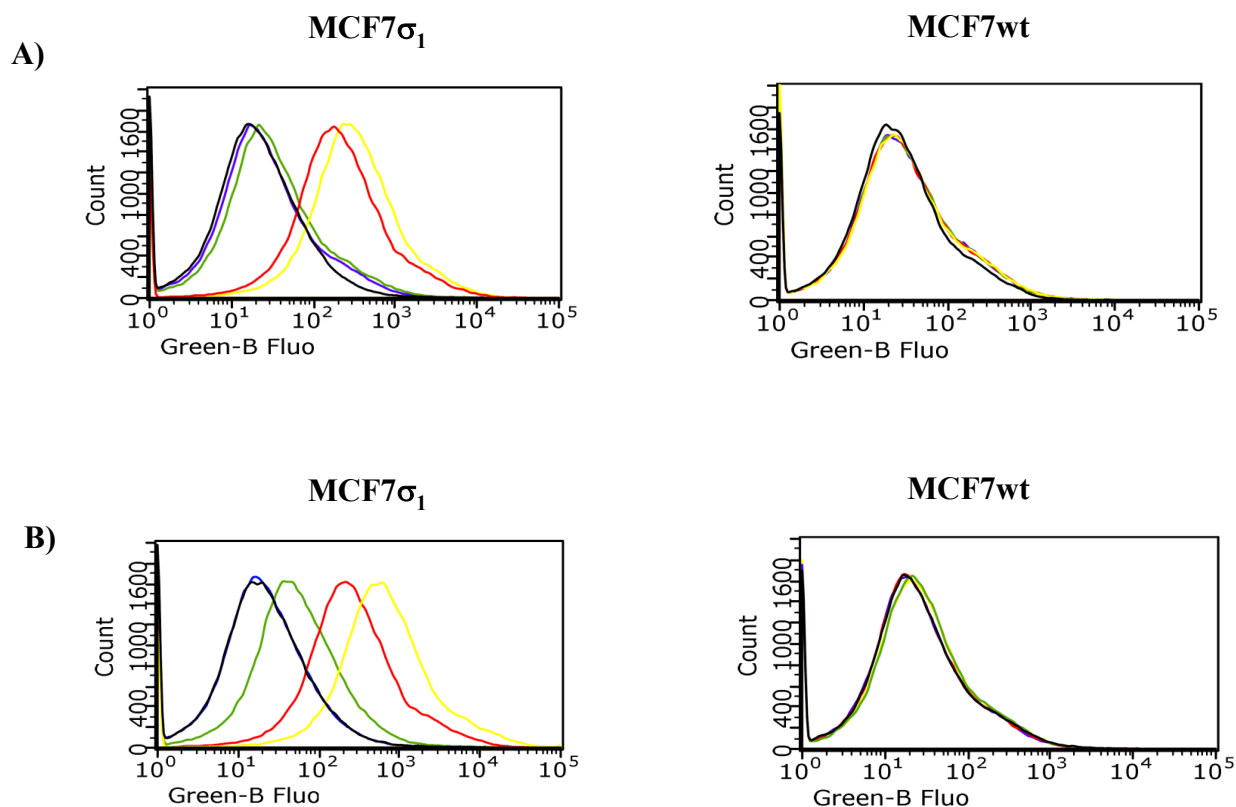


**Figure 4.** Flow Cytometry analysis (cell associated fluorescence vs cell count) of MCF7 $\sigma_1$  and MCF7wt, exposed to compound **5** or **6** and treated with compound **10** (10  $\mu$ M) to mask  $\sigma_2$  receptors, or (+)-pentazocine (10  $\mu$ M) to mask  $\sigma_1$  receptors, or both **10** (10  $\mu$ M) with (+)-pentazocine (10  $\mu$ M). A) Displacement of **5** (100 nM, yellow curve): black curve: control; red curve: 10  $\mu$ M **10**; green curve: 10  $\mu$ M (+)-pentazocine; violet curve: 10  $\mu$ M **10** with (+)-pentazocine 10  $\mu$ M. B) Displacement of **6** (100 nM, yellow curve): black curve: control; red curve: 10  $\mu$ M **10**; green curve: 10  $\mu$ M (+)-pentazocine; violet curve: 10  $\mu$ M **10** with (+)-pentazocine 10  $\mu$ M.

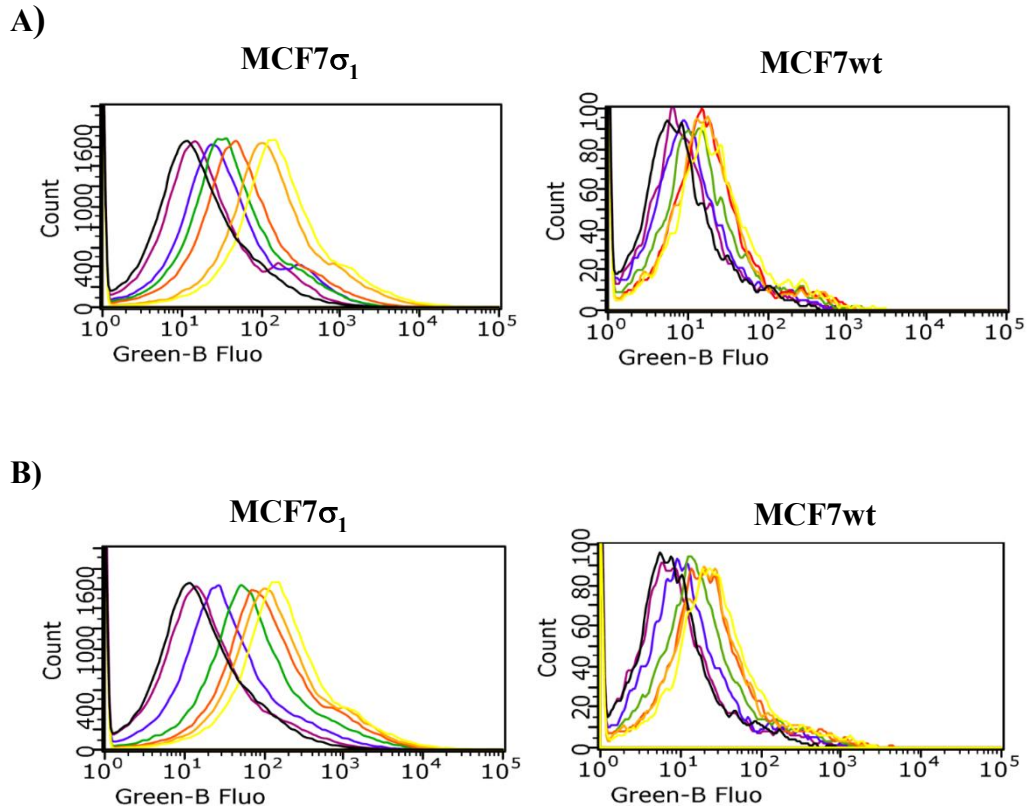


**Figure 5.** Flow Cytometry analysis (cell associated fluorescence vs cell count) of MCF7 $\sigma_1$  and MCF7wt, exposed to **5** and treated with **10** (10  $\mu$ M) to mask  $\sigma_2$  receptors. A) Displacement of **5** (100 nM, yellow curve) with increasing concentrations of PB190: black curve: control; orange curve: 1 nM PB190; red curve: 10 nM PB190; green curve: 100 nM PB190; blue curve: 1  $\mu$ M PB190; violet curve: 10  $\mu$ M PB190. B) Displacement of **5** (100 nM, yellow curve) with increasing concentrations of PB212: black curve: control; orange curve: 1 nM PB212; red curve: 10 nM PB212; green curve: 100 nM PB212; blue curve: 1  $\mu$ M PB212; violet curve: 10  $\mu$ M PB212.

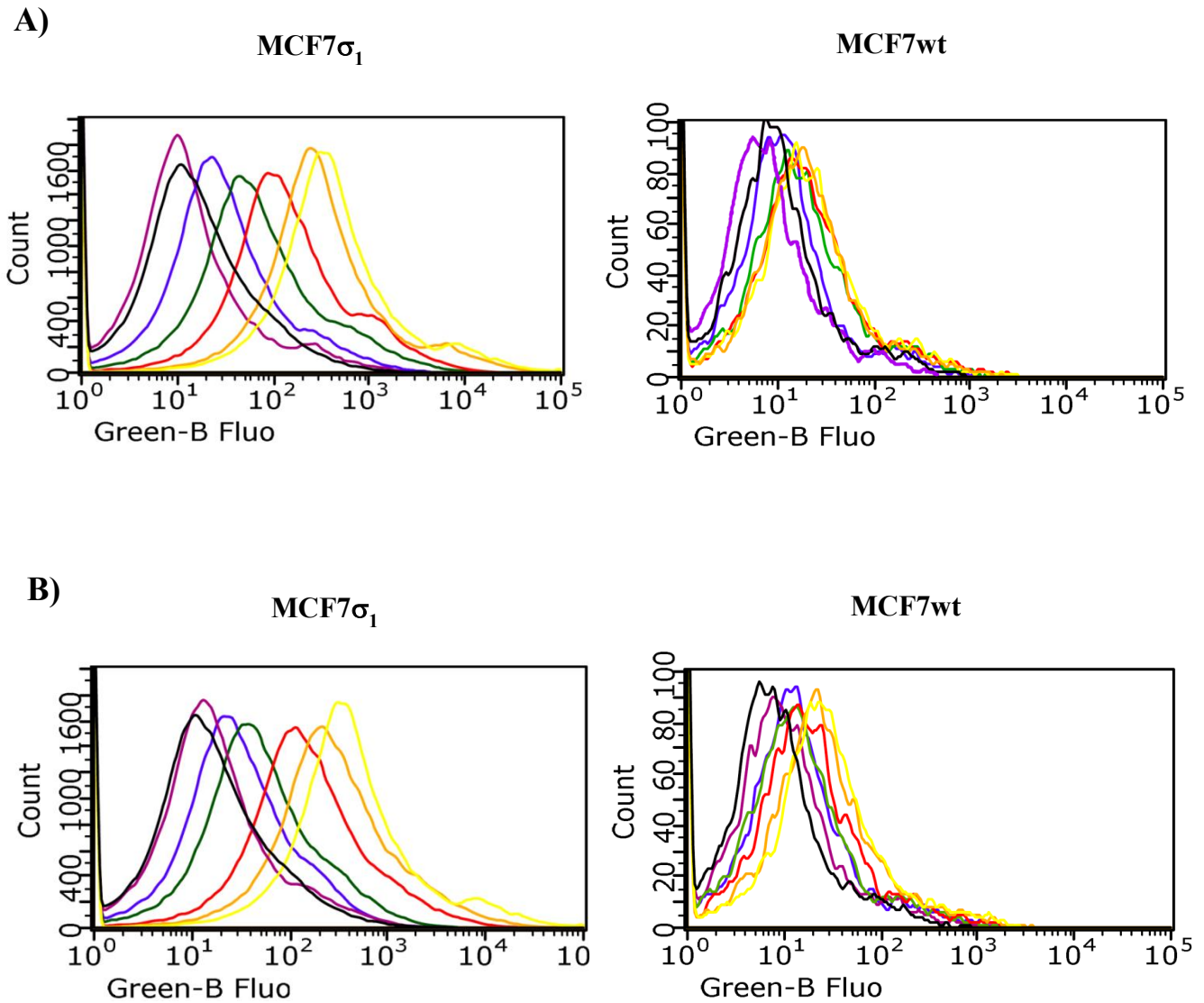


**Figure 6.** Flow Cytometry analysis (cell associated fluorescence vs cell count) of MCF7 $\sigma_1$  and MCF7wt, exposed to **6** and treated with **10** (10  $\mu$ M) to mask  $\sigma_2$  receptors. A) Displacement of **6** (100 nM, yellow curve) with increasing concentrations of PB190: black curve: control; orange curve: 1 nM PB190; red curve: 10 nM PB190; green curve: 100 nM PB190; blue curve: 1  $\mu$ M PB190; violet curve: 10  $\mu$ M PB190. B) Displacement of **6** (100 nM, yellow curve) with increasing concentrations of PB212: black curve: control; orange curve: 1 nM PB212; red curve: 10 nM PB212; green curve: 100 nM PB212; blue curve: 1  $\mu$ M PB212; violet curve: 10  $\mu$ M PB212.

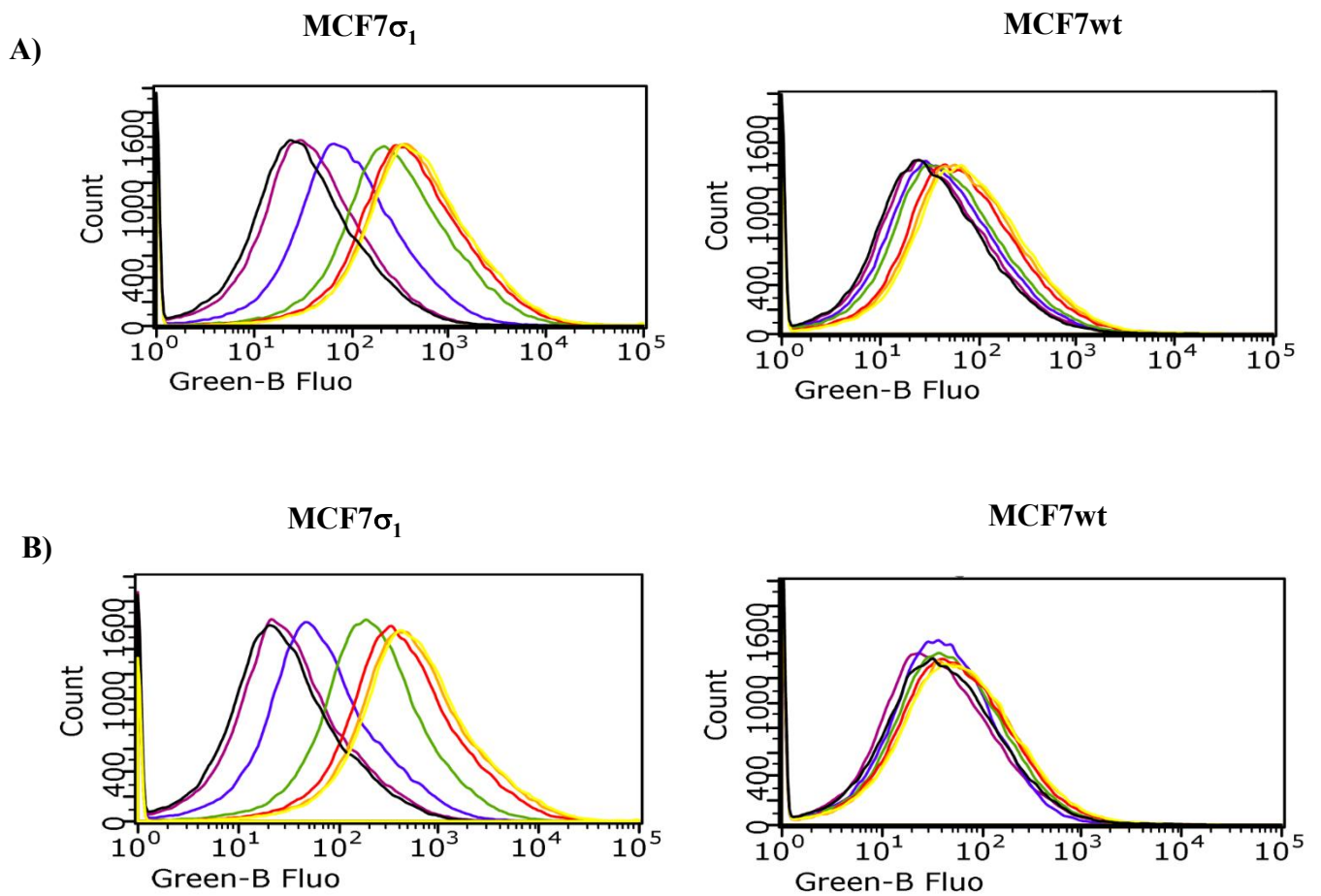
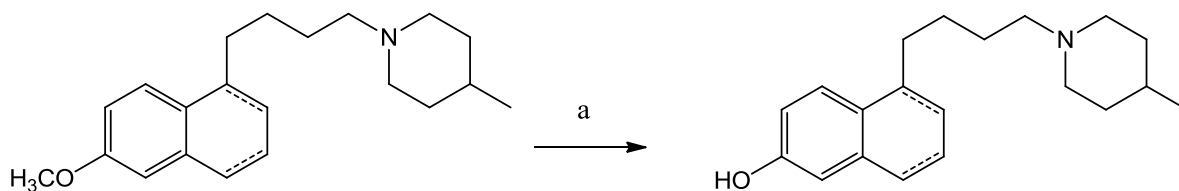
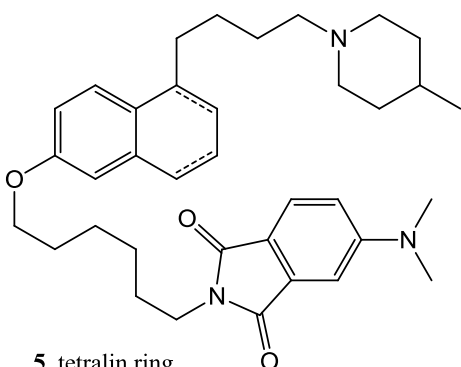


**Figure 7.** Flow Cytometry analysis (cell associated fluorescence vs cell count) of MCF7 $\sigma_1$  and MCF7wt, exposed to **5** or **6** and treated with **10** (10  $\mu$ M) to mask  $\sigma_2$  receptors. A) Displacement of **5** (100 nM, yellow curve) with increasing concentrations of (+)-pentazocine: black curve: control; orange curve: 1 nM (+)-pentazocine; red curve: 10 nM (+)-pentazocine; green curve: 100 nM (+)-pentazocine; blue curve: 1  $\mu$ M (+)-pentazocine; violet curve: 10  $\mu$ M (+)-pentazocine. B) Displacement of **6** (100 nM, yellow curve) with increasing concentrations of (+)-pentazocine: black curve: control; orange curve: 1 nM (+)-pentazocine; red curve: 10 nM (+)-pentazocine; green curve: 100 nM (+)-pentazocine; blue curve: 1  $\mu$ M (+)-pentazocine; violet curve: 10  $\mu$ M (+)-pentazocine.

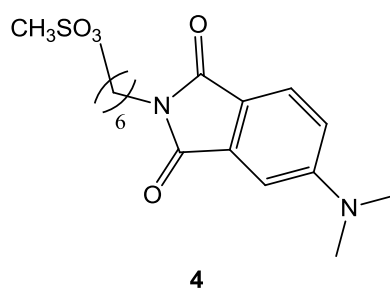


**PB190**, tetralin ring  
**PB212**, naphthalene ring

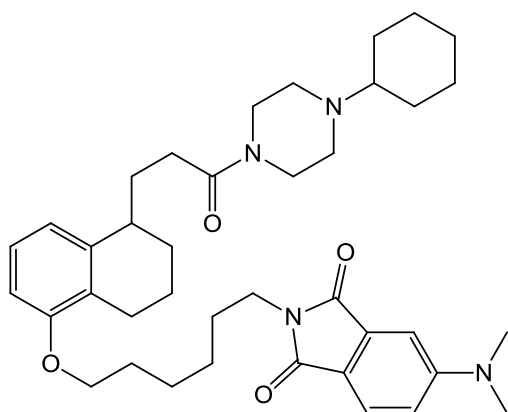
**2**, tetralin ring  
**3**, naphthalene ring



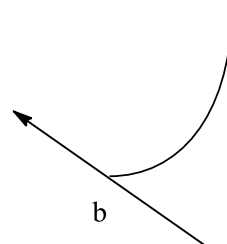
**5**, tetralin ring  
**6**, naphthalene ring



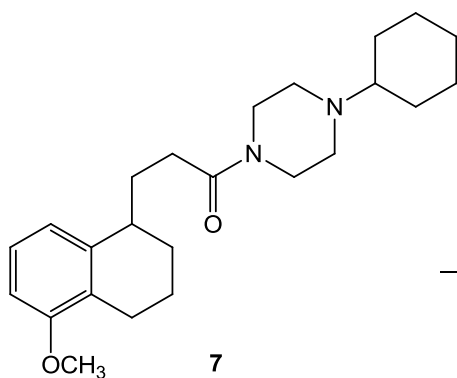
**4**



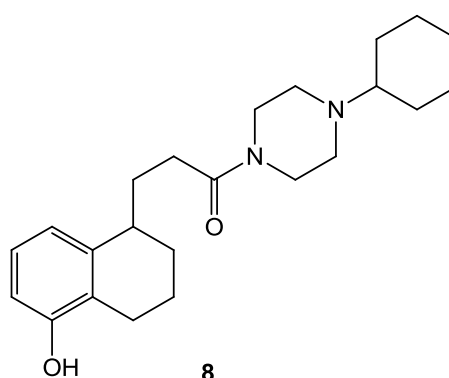
**9**



**b**



**7**



**8**

**Scheme 1.** Reagents and Conditions: (a)  $\text{BBr}_3$ ,  $\text{CH}_2\text{Cl}_2$ , from  $-78^\circ\text{C}$  to room temperature, overnight; (b)  $\text{K}_2\text{CO}_3$ , DMF,  $150^\circ\text{C}$ , overnight.

## Supporting Information

### Development of sigma-1 ( $\sigma_1$ ) Receptor Fluorescent Ligands as Versatile Tools to Study $\sigma_1$ Receptors

Carmen Abate,<sup>\*,a</sup> Chiara Riganti,<sup>b</sup> Maria Laura Pati,<sup>a</sup> Dario Ghigo,<sup>b</sup> Francesco Berardi,<sup>a</sup> Timur Mavlyutov,<sup>c</sup> Lian-Wang Guo,<sup>c</sup> Arnold Ruoho<sup>d</sup>

<sup>a</sup>*Dipartimento di Farmacia-Scienze del Farmaco, Università degli Studi di Bari ALDO MORO, Via Orabona 4, I-70125 Bari, Italy*

<sup>b</sup>*Department of Oncology, University of Turin, via Santena 5/bis, 10126, Torino, Italy*

<sup>c</sup>*Department of Surgery, School of Medicine and Public Health, University of Wisconsin, Madison, USA*

<sup>d</sup>*Department of Neuroscience, School of Medicine and Public Health, University of Wisconsin, Madison, USA*

Table of contents (total of 3 pages)

Physical Properties and Elemental Analyses, Page 2.

Figure 1, Page 3;

Figure 2, Page 4;

Comp.	Formula <sup>a</sup>	Calculated			Found			mp, °C
		C	H	N	C	H	N	
<b>5</b>	$C_{36}H_{51}N_3O_3 \cdot C_2O_4H_2 \cdot \frac{1}{2}H_2O$	67.83	8.09	6.25	67.74	8.00	6.3	105–107 <sup>b</sup>
<b>6</b>	$C_{36}H_{47}N_3O_3 \cdot HCl \cdot 1.75H_2O$	67.80	8.14	6.59	67.84	7.75	6.67	97–99 <sup>b</sup>
<b>9</b>	$C_{39}H_{54}N_4O_4 \cdot 2HCl$	65.44	7.89	7.83	65.19	7.89	7.79	140–143 <sup>b</sup>

**Table of Physical Properties and Elemental Analyses**

<sup>a</sup>Elemental analyses were within  $\pm 0.4\%$  of the theoretical values for the formulas given.

<sup>b</sup>Recrystallized from MeOH. <sup>c</sup>Recrystallized from MeOH/Et<sub>2</sub>O.

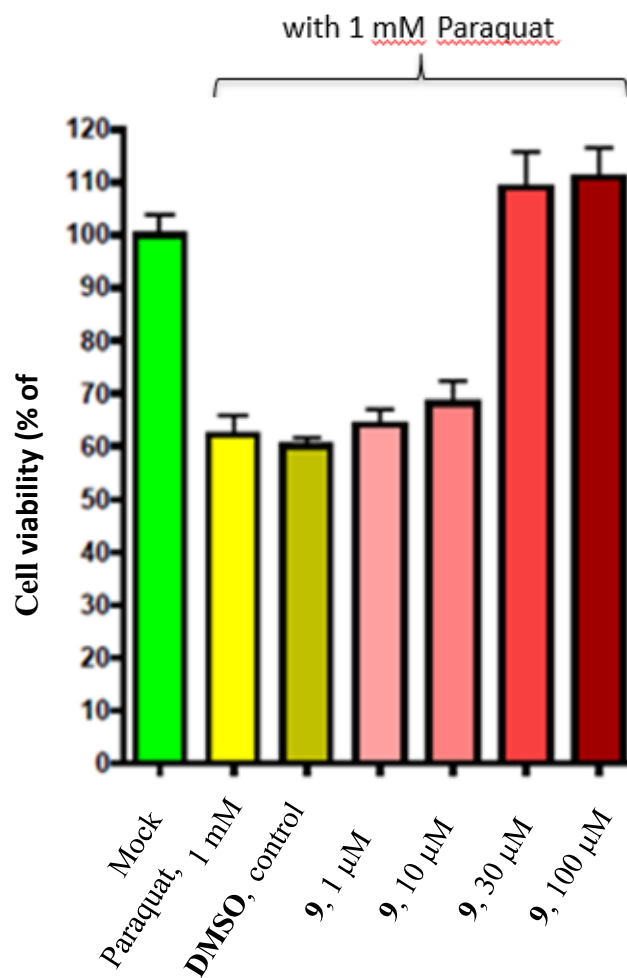


**Figure 1.** Compound **9** protected  $\sigma_1$  receptor against paraquat-mediated toxicity in concentration-dependent manner protects as estimated by a MTT assay in ARPE19 cells. All drugs were applied simultaneously for 24 hours.

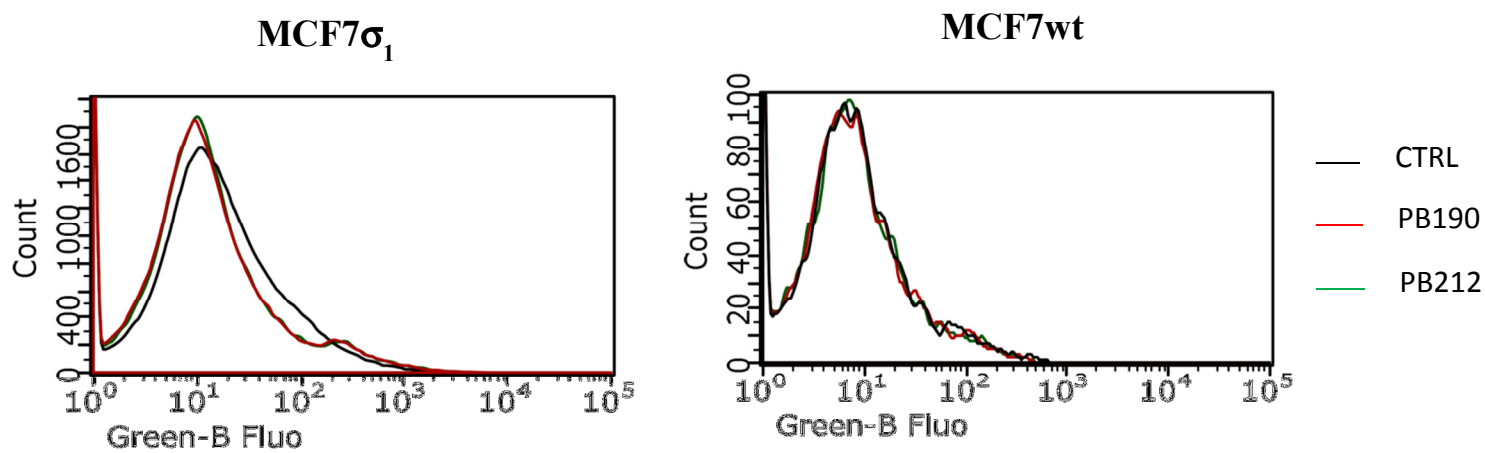


**Figure 2.** Basal fluorescence in MCF7 $\sigma_1$  or MCF7wt in the presence of PB190 or PB212 (10  $\mu$ M, 75 min), masking  $\sigma_2$  receptors with compound **10**.